

Gray-Level Co-occurrence Matrix Bone Fracture Detection

HUM YAN CHAI¹, LAI KHIN WEE^{1,2}, TAN TIAN SWEE¹, SHEIKH HUSSAIN¹

¹ Department of Biomedical Instrumentation and Signal Processing

Faculty of Health Science and Biomedical Engineering

Universiti Teknologi Malaysia

UTM Skudai, 81310 Johor

MALAYSIA

² Institute for Biomedical Engineering and Informatics

Faculty of Computer Science and Automation

Technische Universität Ilmenau

POB 100565, 98684 Ilmenau

GERMANY

yechum2@live.utm.my, kwlai2@live.utm.my, tantswee@utm.my <http://www.fkbsk.utm.my/>

Abstract: - Fractures of bone are a common affliction in orthopedic wards at any given time. Trained radiologists generally identify abnormal pathologies including fractures with a relatively high level of accuracy. However studies examining reader accuracy have shown that in some cases the miss rate can be as high when reading x-rays containing multiple abnormalities. Accurate diagnosis of fractures is vital to the effective management of patient injuries. As a result, detection of long-bone fractures is an important orthopedics and radiologic problem, and it is proposed that a novel computer aided detection system could help lowering the miss rate. This paper examines the development of such a system, for the detection of long-bone fractures. This project fully employed MATLAB 7.8.0 (.r2009a) as the programming tool for loading image, image processing and user interface development. Results obtained demonstrate the performance of the femur's long bone fracture detection system with some limitations.

Key-Words: - texture analysis, bone fracture, classification, gray-level co-occurrence matrix, image processing

1 Introduction

Since x-rays were invented in 1895 by Wilhelm Conrad Roentgen, a German scientist, it has been used as a main medical imaging modality especially in orthopedic diagnosis due to the fact that it is a relatively safe method of investigation as the radiation exposure is relatively low.

Today, a large number of x-ray images are interpreted in hospital and computer aided system that can perform some intelligent task and analysis is needed in order to raise the accuracy and bring down the miss rate in hospital. Conventionally, doctors in hospital examine the bone x-ray images based on their experience and knowledge whether a fracture exist. These kinds of manual inspection of x-rays consume a lot of time and the process itself is monotonous and mistakes might be made during the inspection.

Since detection of fractures is an important orthopedics and radiologic problem, and therefore it is proposed that our novel CAD system could improve the current manual inspection of x-ray images system.

This paper discusses the development of such a system which can differentiate the fractured bone from the non-fractured bone. Other objective includes

classification of specific type of fractured femur. This paper will focus on femur shaft fracture detection.

Femur is the longest and the strongest bone in the skeleton in our human body. It is not vertical in the erect posture and is separated above from its fellow by an interval corresponding to the breadth of the pelvis, but inclining gradually downward and medial ward, near the line of gravity of the body. The Inclination mentioned is not identical in all people, and is greater in the female. Like other long bones, the femur is divisible into three main parts, which are the body (Diaphyseal) and the two extremities.

The fractures of the femur's Diaphyseal will only occur during serious incident. These fractures often happen in the same extremity including the fractures of the femoral neck, posterior fracture-dislocation of the hip, tears of the collateral ligaments of the knee and osteochondral fractures involving the distal femur or patella and fractures of the tibia. It is significant to examine the joint above and the joint below fracture. Films of the uninjured Femur are useful for selecting the correct internal fixation device. [1]

The fracture of the diathesis of femur can be classified first into three group which are Simple, Wedge and

Complex. For simple fracture, it will be classified into three groups which are spiral, oblique and transverse. For wedge fracture, it will be further classified into spiral wedge, Bending wedge, Fragmented wedge. For complex fracture, it will be classified into Spiral, segmental and irregular. [2]

Our ultimate aim is to produce and design a gray level co-occurrence matrix based computer algorithm system with user graphical interface that able to analyze a mid-shaft fracture of a long bone, highlight suspected regions of the x-ray image, and detect the fracture of femur if it exists.

Tian et al. [3] has implemented the method of detecting femur fractures in x-ray images by computing the angle between the shaft axis and the neck axis. However this kind of method can only works on those fractures which are severe and has a significant change in the angle of the neck and shaft of the femur. This type of fracture detection using angle measurement has limitation in detecting the other type of fractures like wedge and simple.

Martin Donnelley et al. [4] have created a CAD system for the long bone fracture detection. The system contain of four stages which are Long bone edge detection using scale-space approach, parameter approximation using the normal parameterization of the Hough transform and therefore spatially extended patterns were transformed into spatially compact features within the space of possible parameter values (ρ , θ), Diathesis segmentation using the long-bone approximation parameters (ρ_i , θ_i) to calculate the best estimate of the bone centre-line, Fracture detection using gradient analysis.

T. Link, S. Majumdar et al. [5] had constructed first and higher order texture like mean and standard deviation and parameters such as apparent mineralization and total area associated with the strength regions are derived for normal and abnormal images. The statistically derived significant parameters corresponding to the primary strength regions are fed to the neural network for training and validation.

X. Ouyang [6] et al. had proposed texture analysis of spinal trabecular bone structure by using higher order statistic analysis. [7] A. Materka et al bone mineral density estimated by means of dual-photon absorptiometry (DXA) based on co-occurrence matrix texture analysis by computing the standard DXA technique and the image mean, standard deviation, skewness, kurtosis, energy, entropy, fractal dimension in vertical dimension, and variance-based fractal dimension and examine their correlations.

J. Veenland [8] suggested that the power of texture parameters is corrected for the influence of BMD to determine the additional information indicated by these parameters since in radiographs density and structure are strongly correlated. The predictive power of these texture

parameters are obtained through the Grey-Level Dependence Method and the Morphological Gradient Method by examining Correlation coefficients of the investigated texture parameters.

In the present method, we presented a novel CAD system which could improve the current manual inspection of x-ray images system. The rest of this paper is organized as follows. In section 2, we describe the procedure of software development, system design and the detection procedure of bone fracture. The results of present method are shown in Section 3, and finally we draw some conclusions in Section 4.

2 Material and Methods

In this section, we describe the overall system design, image pre-processing techniques, segmentation, results analysis and classification. Figure 1 shows the block diagram of our developed algorithm. The input of X-Ray femur images, in DICOM 3.0 standard format will be interpreted into the developed software. The tested X-ray images were taken at 53 kV and 4 mAs, and were digitized at 7 bit/pixel using a CCD camera. Based on the tags information from the header metadata, the size of the processed images are in 410 x 500 resolutions.

2.1 System Design

Due to the nature of X-Ray image restoration, some image preprocessing techniques are necessary to eliminate the noise and image artifacts. The image pre-processing steps are including binary conversion, fine particles elimination and bone shaft detection. For the sake to ease the processes above, and make it easier to be understood, the input image will be transformed into binary form for the very first. It follows by the K means based programming technique to detect the shaft area of the femur bone. Once the region of this specific area been identified, it will be cropped and recognize as region of interest for further segmentation application.

In order to detect the fracture bone, edge of bone features appears as a vital rule for the classification task. A wide conventional of edge detector have been considered, such as Sobel and Canny techniques have a shortcoming in border energies calculation, as more than two interest plotlines will be mapped within the output image. Thus, we have developed our own unique algorithm using shaft to obtain the edge. The thinnest width and thickest width will be used as the parameters for the reconstruction of region-of-interest. Lastly, the resultant region will be undergoing computerized texture analysis using GLCM, where it will be compared with threshold value in order to carry out the classification.

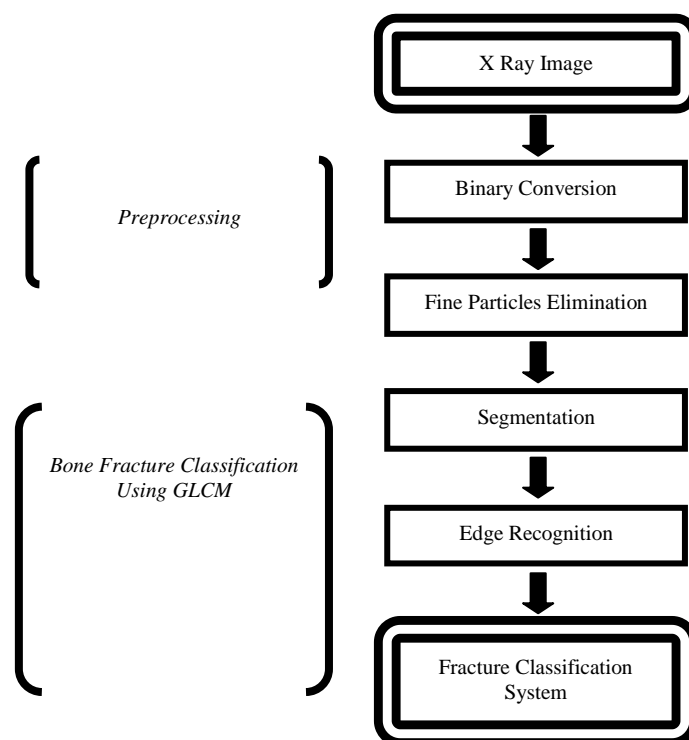


Fig. 1 System block diagram

2.2 Image Pre-processing

2.2.1 Binary Conversion

The image is changed to binary to ease the computing process and maximize the speed of calculating due to the rapid Boolean operators. By changing to binary, the femur shaft can be separated from the soft tissue shade which can be considered noise during the bone shaft image processing.

The digital x-ray images which contain an array of discrete value called intensities. Each gray level is quantized into a set of numbers represented by number of bits. In the case of binary, only one bit is assigned to each pixel. '0' represents black pixel and '1' represents white pixel. However this binary conversion needs to undergo a thresholding process.

The process of thresholding can be illustrated as a quantization in gray level or it can be treated as an algorithm that involve against a function. The process can also be viewed as a simple comparison operation as well. Suppose threshold value, H within the grayscale image intensities from E, E+1, E+2 ...to F, each pixel value is compared to H and decision is made to define a new pixel value which is either zero or one of the corresponding pixel in the output binary image.

Suppose the output image A, and the input image is B and N is the image pixel array.

The comparison operator is shown below:

$$A(N) = \begin{cases} '0' & \text{if } B(N) \geq H \\ '1' & \text{if } B(N) < H \end{cases} \quad \text{for } N = E \rightarrow F \quad (1)$$

The threshold value is of extremely significance and need to be carefully selected. The quality of the image depends heavily on this threshold value.

2.2.2 Bone Border Edge detection

The bone border will be detected using Laplacian edge detector by operating a Laplacian operator convolution with the image [9]. This involve a few steps. First the image is convolved with the Gaussian operator with the intent of blurring the image since not every edge is needed, only the border edge, then the Laplacian operator will be performed on the blurred image:

$$F(x, y) = -|\nabla(G_\sigma(x, y) * I(x, y))|^2 \quad (2)$$

Where,

$$\nabla^2 f = \frac{\partial^2 f}{\partial x^2} + \frac{\partial^2 f}{\partial y^2}$$

Where $G_\sigma(x, y)$ is a two-dimensional Gaussian function with standard deviation σ and ∇ is the gradient operator, ∇^2 is the laplacian operator.

2.2.3 Fine particles eliminations

By using the median filter algorithm, the target pixel's value is replaced by the median value of the neighboring

pixel in a kernel. The kernel's is of importance in determining output image. These are the algorithm parameters that should carefully chosen depends on the image fine particles. The median filter is the filter chosen after the edge detector due to its ability to suppress isolated noise while preserving the femur bone border edge.

2.3 K-means based shaft segmentation

By using K-means unsupervised clustering technique [11], the femur x-ray image will be clustered into two groups which are the shaft and the non-shaft area with the 'K' value equals to two. The purpose of this algorithm can be achieved by minimizing an *objective function*, in this case a squared error function, as shown in Equation (3).

$$\sum_{j=1}^K \sum_{i=1}^n ||x_i^{(j)} - c_j||^2 \tag{3}$$

Where $||x_i^{(j)} - c_j||^2$ is the distance measurement between the data point $x_i^{(j)}$ and the cluster center c_j , it indicates the distance difference from the data point to the cluster centre. In this paper, the data point mentioned represents the number of white pixels which contain the value equal to one in each horizontal direction of the binary image.

A few steps will be used in designing the algorithm. First, two cluster centre will be chosen randomly amidst the data points followed by constructing the distance

difference between each data point and the cluster centre. After that, each data point will be assigned to one of the two clusters centre depends on the distance difference. When all the data points are assigned to cluster centre, the new cluster centre is then recalculated by computing the mean of each cluster group. These steps will keep repeating itself until the cluster centre no longer change. By then, the objective function reaches its minimum value.

In other words, each data points had been assigned to one of the two clusters so as to minimize a measure of dispersion within the clusters. All the pixels that belong to the cluster centre which contains the lower value are considered as the shaft of the femur and therefore the cluster centre has become an unsupervised threshold value that can differentiate the femur's shaft from non-shaft area.

2.4 Grey Level Co-occurrence Matrixes

Since the GLCM were proposed by Haralick [10], it has been utilized as the main tool in image texture analysis. Haralick suggested statistics equations that can be calculated from the co-occurrence matrix and be used in describing the image texture. It is a statistical way to indicate image texture structure by statistically sampling the pattern of the grey-levels occurs in relation to other grey levels. There are mostly weighted averages of the normalized co-occurrence matrix contents by multiplying a weighted average multiplier with the intent of expressing the relative significance of the value. Figure 2 below shows the fundamental of N x N matrix.

$$\begin{pmatrix} P(1,1) & P(1,2) & P(1,3) & \dots & \dots & P(1,N) \\ P(2,1) & P(2,2) & \dots & \dots & \dots & \dots \\ P(3,1) & \dots & \dots & \dots & \dots & \dots \\ \dots & \dots & \dots & \dots & \dots & \dots \\ \dots & \dots & \dots & \dots & \dots & \dots \\ P(N-1,1) & \dots & \dots & \dots & \dots & \dots \\ P(N,1) & P(N,2) & \dots & \dots & \dots & P(N,N) \end{pmatrix}$$

Fig. 2 The fundamental of N x N matrix forms

The matrix shown above is squared with dimension N which represents the number of gray levels in the image. Element $[i, j]$ of the matrix is generated by computing the frequency of a single pixel with value i is adjacent to the pixel with value j and then divide the matrix by the total number of such comparisons made. Each value in the matrix is hence become the probability that a pixel with value i which will be found adjacent to a pixel of value j .

The mentioned co-occurrence matrix features formula which computed from the Image (i, j) are;

Angular Second Moment,
 $(ASM) = \sum_{i,j=0}^{N-1} P_{i,j}^2 \tag{4}$

The image energy is the square root of ASM which is a very useful second order texture statistical operator that able to measure the uniformity of the targeted window

from image. Each element in the co-occurrence matrix in Figure 2 is squared and summed up. If in the case of a uniform image which has been normalized and all the pixels values equals to '1', the output of this operator is equals to '1', if the uniform image is not normalized, the output value equals to the number of the window's size. Recall that Normalization changes the number of combination into a probability value range from zero to one. In Figure 2, all the value has been normalized, therefore the element is $p(i, j)$ which is a probability.

$$\text{Energy} = \sqrt{\sum_{i,j=0}^{N-1} P_{i,j}^2} \tag{5}$$

$$\text{Contrast} = \sum_{i,j=0}^{N-1} P_{i,j}(i,j)^2 \tag{6}$$

The diagonal elements of the matrix shown in Figure 2 indicates the group of pixel which has no difference in pixel value, For instant, the first element $p(1, 1)$, shows that the probability of the combination of two pixels in certain spatial relation which are of the same value equals to '1', the second element represents the probability of the combination of two pixels in certain spatial relation which are of the same value equals to '2' and so on. In other words, it shows no contrast in diagonal elements in the co-occurrence matrix. Therefore if the intent is to measure the contrast of the texture which the matrix represented, weights need to be created so that the output value of equation (4) shows larger value accordingly with the degree of contrast with the fact that the contrast increases as the distance of elements in the matrix from the diagonal increases. For example the element $p(1, N)$ and $p(N, 1)$ should show much lower value of contrast compared to the element $p(1, 3)$, $p(2, 2)$ in Figure 2.

$$\text{Dissimilarity (DIS)} = \sum_{i,j=0}^{N-1} P_{i,j}|i - j| \tag{7}$$

$$\text{GLCM correlation} = \sum_{i,j=0}^{N-1} P_{i,j} \left[\frac{(i-\mu_i)(i-\mu_j)}{\sqrt{(\sigma_i^2)(\sigma_j^2)}} \right] \tag{8}$$

The GLCM correlation indicates the linear dependency of the linear dependency between the grey levels and the neighboring pixels where μ_i represents the horizontal mean in the matrix, μ_j represents the vertical mean in the matrix, σ_i^2 and σ_j^2 represents dispersion around the mean of combinations of target and neighbor pixel.

$$\begin{aligned} \text{GLCM Mean} &= \mu_i = \sum_{i,j=0}^{N-1} i(P_{i,j}) \\ &= \mu_j = \sum_{i,j=0}^{N-1} j(P_{i,j}) \end{aligned} \tag{9}$$

$$\begin{aligned} \text{GLCM Variance} &= \sigma_i^2 = \sum_{i,j=0}^{N-1} (i - \mu_i)(P_{i,j}) \\ &= \sigma_j^2 = \sum_{i,j=0}^{N-1} (j - \mu_j)(P_{i,j}) \end{aligned} \tag{10}$$

$$\text{Entropy (ENT)} = \sum_{i,j=0}^{N-1} P_{i,j}(-\ln P_{i,j}) \tag{11}$$

$$\text{Homogeneity (HOM)} = \sum_{i,j=0}^{N-1} \frac{P_{i,j}}{1+(i-j)^2} \tag{12}$$

Where μ_i , μ_j , σ_i , σ_j are the means and Standard Deviations

Homogeneity, also called 'Inverse Difference Moment' is an inversion to the contrast. In calculating the contrast, the weight of element increases when distance of element from diagonal increases. Inversely, while calculating the Homogeneity, the weight of element decreases as the distance of elements from diagonal increases. In short, the weight of contrast (4) is $(i - j)^2$, on the other hand, the weight of Homogeneity is $\frac{1}{1+(i-j)^2}$.

c		d							
						a			
				Target pixel					
		b							
									e

Fig. 3 Distance and direction used in computed matrix

The spatial relationships of pixels can be defined using distance and direction, figure below show the example of how the distance and direction are used in computing the matrix.

The spatial relationship of neighbor pixel 'a' to the target pixel is described as [2,-2] indicates 3 pixel to the East, and 2 pixels to North. The neighbor pixel 'b' to the target pixel is described as [-2, 2] indicates 2 pixel to the West, and 2 pixels to south. The neighbor pixel 'c' to the target pixel is described as [-4,-3] indicates 4 pixel to the west, and 3 pixels to north. The neighbor pixel 'd' to the target pixel is described as [-2,-4] indicates 2 pixel to the West, and 4 pixels to North. The neighbor pixel 'e' to the target pixel is described as [5, 4] indicates 5 pixel to the east,

and 4 pixels to north. This spatial relationship is often referred as offset in GLCM calculation.

3 Result and Analysis

Figure 4 shows part of our experimental results using sample patients' data and the obtained findings demonstrated that the state of the art of computerized GLCM method is able to produce accurate border in most of the samples. Figure 5 shows the resultant image conversion into binary form, where the value 0 represents black pixel and value 1 represents the white pixel in the image.

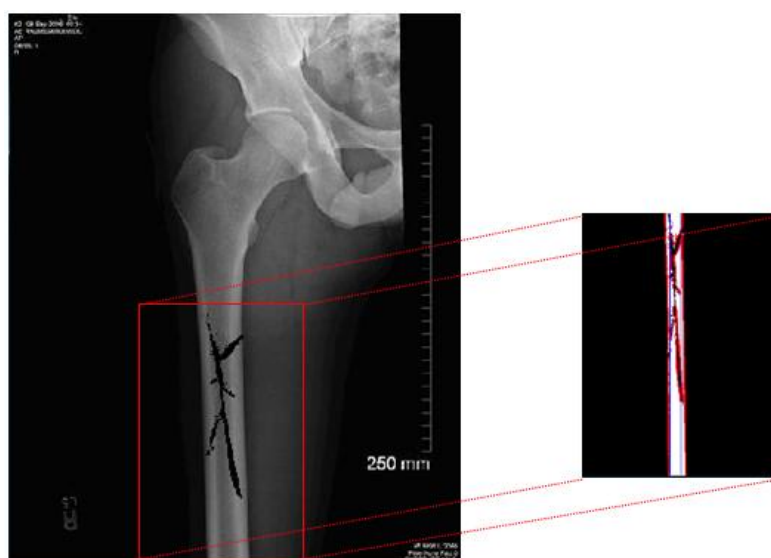


Fig. 4 Experimental result of bone fracture tracking



Fig. 5 X-ray image in binary form

Figure 6 shows that a blue line is drawn to separate the shaft and epiphysis of femur. The algorithm enable each horizontal line of the picture inspects and identifies the white pixel among each row of pixels. When the white pixels of certain horizontal line exceed a threshold value, it will sketch a line to distinguish the shaft and the upper

epiphysis of femur. After filtering the image, the image will be processed to get the edge and a red dot will be drawn on each point of edge detected as shown in Figure 8.

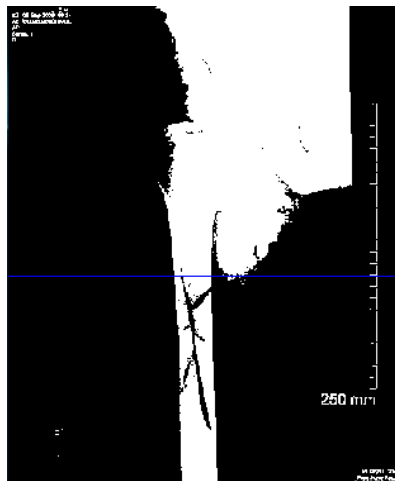


Fig. 6 Separation of shaft and upper epiphysis of femur

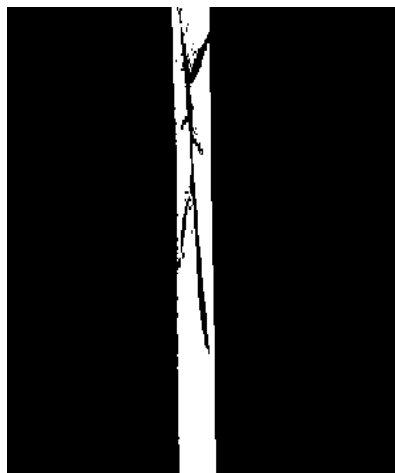


Fig. 7 Filtered image



Fig. 8 Edge-detected image

After that, the middle point the shaft will be calculated using the average of the width of the thinnest part of the shaft and the thickest part of the shaft. After obtaining the middle point, each middle point will be extended to left

and right according to the shaft size as shown in Figure 9. The areas within both blue lines represent the region-of-interest of our later GLCM measurement.

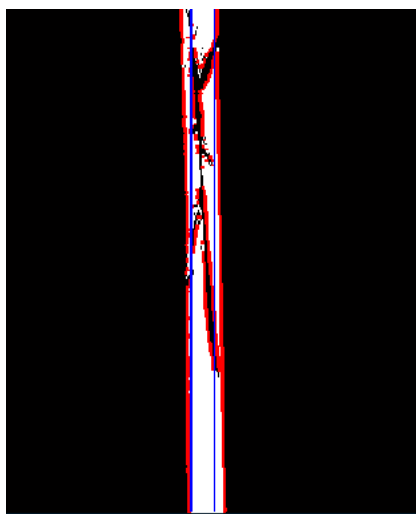


Fig. 9 Region-of-interest image

3.1 GLCM Calculation of Fractured and non-fractured Femur

The region- of- interest of the femur x-image contain Fractures will be the region will undergo GLCM for every 50 pixel length and the length depends on the width of the size of shaft. The area will be scanned and obtain the GLCM values, for the image that 500 x 400.

For each area, there will be four statistical GLCM values calculated ,in four directions which are [1,0], [0,1], [1,1], [-1,-1], Only the average of the four directions will be taken and therefore for every area there will be total 4 values. Energy provides the sum of squared elements in the GLCM also known as uniformity or the angular second moment. The values of energy indicate the texture of the area, if it is equal to 1, it means the area is uniform and no fracture found and vice versa. Contrast measures the local variations in the gray-level

co-occurrence matrix. Correlation measures the joint probability occurrence of the specified pixel pairs. Homogeneity measures the closeness of the distribution of elements in the GLCM to the GLCM diagonal.

After obtaining the statistical value of GLCM, four statistical values which are contrast, correlation, Energy, Homogeneity will be analysed. The algorithm itself will calculate the value compare and classified automatically and indicate to the user the area of fracture if any exist.

In order to access the performance and usefulness of the developed system in a real application, a thorough evaluation of the method was carried out at the Biomedical Research Centre, Universiti Teknologi Malaysia, Malaysia. We ran the algorithm on a set of X-Ray images (n = 30), with 410 x 500 sized resolutions for performance evaluation. The images were cataloged into two different testing groups of k_1 and k_2 respectively.

Table 1 – PERFORMANCE OF DEVELOPED ALGORITHM FOR BONE FRACTURE CLASSIFICATION

Threshold	Group k_1	Group k_2	Accuracy
threshold > 0.95	12 true-positive (TP)	1 false-positive (FP)	86.67%
threshold < 0.95	3 false-negative (FN)	14 true-negative (TN)	
Total	15	15	

$$Accuracy = (TP + TN) / (TP + TN + FN + FP)$$

Each group of testing catalogue consisted of 15 numbers of X-Ray images. The first group k_1 were images shows normal femur bone screening, where the second group of images k_2 were femur bone images with fracture found. Table 1 lists the performance of developed software on k_1 and k_2 groups of images.

Simulations result shows that the developed algorithm is capable achieving as high as accuracy about 86.67 percent and able to provide reliable and consistent findings.

Based on equations 13, 14, 15 and 16 the calculated sensitivity was 80 percent (12 out of 15), the specificity was 93.33 percent (14 out of 15), the positive predictive value was 92.31 percent (12 out of 13) and the negative predictive value was 82.35 percent (14 out of 17). These results indicate the developed diagnostic model making well recognition and detection of bone fracture.

$$\text{Sensitivity} = TP / (TP + FN) \quad (13)$$

$$\text{Specificity} = TN / (TN + FP) \quad (14)$$

$$\text{Positive Predictive Value} = TP / (TP + FP) \quad (15)$$

$$\text{Negative Predictive Value} = TN / (TN + FN) \quad (16)$$

4 Conclusion

We have proposed a method for automated femur bone fracture detection using GLCM computerized techniques. From this method we are able to classify the absence and presence of bone fracture based on the obtained parameter value from GLCM value. The threshold bordering the absence and presence of bone fracture is set to a value of 0.95. The accuracy of the developed algorithm is achieved at least 86.67 percent which promises an efficient method to recognize bone fracture automatically. Findings show that the system is able to provide consistent and reproducible results.

ACKNOWLEDGMENTS

The authors would like to express our thanks to Universiti Teknologi Malaysia and the Ministry of Higher Education of Malaysia for supporting and funding this study under Zamalah/Institutional Scholarship. Our appreciation also goes to the *Centre of Biomedical Engineering* members for their ideas and comments on this paper.

AUTHOR BACKGROUND

Hum Yan Chai is a present PhD Candidate in the field of Biomedical Engineering in Universiti Teknologi Malaysia (UTM). He is working as Research Member in *Centre of Biomedical Engineering*, Universiti Teknologi

Malaysia. His research interests are X-Ray imaging, medical image processing, filter design, fuzzy logic, and medical computing and performance optimization.

Lai Khin Wee is a present PhD Candidate in the field of Biomedical Engineering in Universiti Teknologi Malaysia (UTM). Currently he is conducting his PhD research at Technische Universitat Ilmenau, Germany. He has been working as Research Associate in "*Progressive Healthcare and Human Development Research Group (PH2D-RG)*", Universiti Teknologi Malaysia. He was actively involved in the Board of Reviewer for more than 12 international Journals and conferences. His research interests are Ultrasound imaging, medical image processing, 3D image reconstruction, signal processing, medical computing and dynamic programming.

Tan Tian Swee received the B.S. degree, M.S. degree and Ph.D. degree in electrical engineering, Universiti Teknologi Malaysia (UTM). Currently, he is working as Lecturer and Research Member in *Centre of Biomedical Engineering*, Universiti Teknologi Malaysia. His research interests include Biomedical Signal Processing, Speech Therapy, Speech Processing, and Medical Electronics.

Sheikh Hussain obtained his first degree in United States in Electronic Engineering. He completed his master's degree at UTM and Ph.D degree in Speech Processing at Edinburgh, UK. Currently he is working as Professor at the Department of Biomedical Instrumentation & Signal Processing, Universiti Teknologi Malaysia. He has published more than 80 papers in international and national conference. His research interests are Heart sound, Infant hearing Screening, Speech Processing.

References:

- [1] Marc F. Swiontkowski, Steven D. Stovitz, "Manual of orthopaedics", pages 330, 2005
- [2] Lippincott Williams & Wilkins, "Orthop Trauma", Volume 21, Number 10 Supplement. Pages 35, 2007
- [3] T. P. Tian, Y. Chen, W. K. Leow, W. Hsu, T. S. Howe, M. A. Png., "Computing neck-shaft angle of femur for x-ray fracture detection", *In Proc. Int. Conf. on Computer Analysis of Images and Patterns (LNCS 2756)*, pages 82–89, 2003
- [4] Martin Donnelley, Greg Knowles, and Trevor Hearn, "A CAD System for Long-Bone Segmentation and Fracture Detection", *Proceedings of the 3rd*

- international conference on Image and Signal Processing*, 2008
- [5] T. Link, S. Majumdar, W. Konermann, N. Meier, J. Lin, D. Newitt, X. Ouyang, P. Peters, , H. Genant, "Texture analysis of direct magnification radiographs of vertebral specimens: Correlation with bone mineral density and biomechanical properties", *Acad. Radiol.*, Volume 4, pages 167–176, 1997
- [6] X. Ouyang, S. Majumdar, T. M. Link, P. A. Y. Lu, J. C. Lin, D. C. Newitt, H. K. Genant, "Morphometric texture analysis of spinal trabecular bone structure assessed using orthogonal radiographic projections", *Medical Physics*, Volume 25, pages 2037–2045, 1998
- [7] A. Materka, P. Cichy, and J. Tuliszkiwicz, "Texture analysis of x-ray images for detection of changes in bone mass and structure", *Texture Analysis in Machine Vision*. World Scientific, 2000
- [8] J. Veenland, T. Link, W. Konermann, N. Meier, J. Grashuis, and E. Gelsema, "Unraveling the role of structure and density in determining vertebral bone strength", *Calcif. Tissue Int.*, Volume 61, pages 474–479, 1997
- [9] S. E. Lim, Y. Xing, Y. Chen, W. K. Leow, T. S. Howe, M. A. Png, "Detection of femur and radius fractures in x-ray images," *2nd Int. Conf. on Advances in Medical Signal and Info.*, 2004
- [10] Robert M. Haralick, "Statistical and structural approaches to texture", *Proceeding of IEEE*, vol. 67, no. 5, pages 786-804, 1979
- [11] J. B. MacQueen, "Some Methods for classification and Analysis of Multivariate Observations", *Proceedings of 5-th Berkeley Symposium on Mathematical Statistics and Probability*", Berkeley, University of California Press, 1:281-297, 1967